

Predicting tumour response to anti-HER1 therapy using medical imaging: a literature review and *in vitro* study of [¹⁸F]-FDG incorporation by breast cancer cells responding to cetuximab

T. A. D. SMITH and R. W. CHEYNE

Aberdeen Biomedical Imaging Centre, School of Medical Sciences, University of Aberdeen, Foresterhill, Aberdeen AB25 2ZD

Accepted: 21 June 2011

Introduction

Epidermal growth factor receptor (EGFR or HER1) is a member of the human epidermal growth factor receptor (HER) tyrosine kinase family which controls cellular events including cell proliferation, differentiation and cell death. Over-expression of HER1 is seen in many tumours, including prostate, colorectal and almost 50% of breast cancers,¹ and is associated with increased metastatic potential and poor prognosis. HER1 ligands including EGF, transforming growth factor- α (TGF α), and heparin-binding EGF and receptor binding induces activation of several intracellular pathways with cellular responses including proliferation, differentiation, motility and metabolism.

The HER family of receptor tyrosine kinases consists of four members (HER1–4). Each consists of an extracellular ligand-binding domain, a transmembrane region and an intracellular tyrosine kinase moiety. Ligand binding to the extracellular domain of HER1 enables its dimerisation with another HER molecule, bringing together their intracellular tyrosine kinase moieties and facilitating cross phosphorylation. Dimers activated by this process then act as activators of the intracellular signalling pathways MAPK/MEK/Erk and PI3K/PKB/Akt.² Increased activation of these pathways has been demonstrated in tumour tissue compared with normal tissue – paired tissue samples from colorectal cancer patients stained with antibodies against EGFR, phospho-EGFR (pEGFR), Akt, pAkt, MAPK and pMAPK were found to have higher levels of pEGFR and its downstream effectors Akt, pAkt, MAPK and pMAPK in cancerous colorectal lesions when compared with normal colorectal tissue.³

A number of anticancer agents have been developed to interfere with HER-activated processes including the small molecules gefitinib and erlotinib, which act at the active site

Correspondence to: Dr. Tim A. D. Smith

School of Medical Sciences, Biomedical Physics Building

Foresterhill, Aberdeen AB25 2ZD, UK

Email: t.smith@abdn.ac.uk

ABSTRACT

Cetuximab, an anti-HER1 (EGFR) antibody, is currently under trial for the treatment of breast cancer. HER1 expression is not necessarily a predictor of response to cetuximab as mutant components of the pathways activated by HER1 which include PI3K/Akt can lead to resistance. Techniques that monitor events downstream of HER1 are more likely to provide an accurate measure of the efficacy of an anti-HER1 treatment. Glucose metabolism has been shown to be strongly influenced by the state of activation of PI3K/Akt. Here, the association between [¹⁸F]-FDG incorporation in breast cancer cells during response to cetuximab is investigated. The study also reviews the development of medical imaging probes that target HER1. The sensitivity to cetuximab of three breast tumour cell lines, SKBr3, MDA-MB-453 and MDA-MB-468, expressing HER1 at low and high levels, are determined using an MTT assay over a six-day period and a clonogenic assay carried out after seven- and 10-day exposures. Incorporation of FDG by cells treated with growth inhibitory doses of cetuximab were carried out after 4 h and two, four and six days of treatment. Glucose transport (rate of uptake of the non-metabolisable analogue [³H]o-methyl-D-glucose), hexokinase activity and lactate production were measured on cells treated with inhibitory doses of cetuximab for six days. The IC₅₀ dose for MDA-MB-468 cells and the IC₁₀ (maximum achievable inhibition) doses for MDA-MB-543 and SKBr3 treated with cetuximab for six days were 2.6, 5 and 148 μ g/mL, respectively. Incorporation of FDG by SKBr3 and MDA-MB-453 cells was found to be decreased by MDA-MB468 cells using IC₅₀ and IC₂₀ doses of cetuximab for six days. Lactate production was found to be increased by MDA-MB-468 cells responding to cetuximab. Incorporation of FDG at the tumour cell level is modulated by treatment with growth inhibitory doses of cetuximab in cells sensitive to cetuximab due to modulation of HK activity.

KEY WORDS: Cetuximab.
Fluorodeoxyglucose F18.
Hexokinase.
Lactic acid.
Positron-emission tomography.

of the tyrosine kinase by competing with ATP.⁴ Antibodies such as cetuximab bind to HER1, preventing interaction with its endogenous ligands, EGF and TGF α , resulting in internalisation of the receptor without causing

phosphorylation of receptor-associated tyrosine kinase.⁵ Binding of cetuximab results in down-regulation of mutant but not wild-type HER1 and inhibition of phosphorylation of MAPK and Akt.⁶ Screening of patients for suitability for treatment with cetuximab currently involves fluorescence *in situ* hybridisation (FISH) to measure *HER1* gene copy number,⁷ or immunohistochemistry (IHC) to detect HER1 protein expression.

However, gene copy number does not always correspond with increased expression of the gene at the protein level. Furthermore, disparity of HER1 expression between different parts of the same tumour and also between a primary tumour and its metastases^{8,9} compromises the reliability of treatment decisions based on determining receptor status on biopsied material taken only from the primary tumour. Detection of tracers targeted to HER1 using medical imaging techniques enables a global approach to HER1 status assessment, facilitating determination of HER1 density averaged over all cells within each detectable lesion. Consequently, the development and application of imaging agents that target HER1 that can be detected using medical imaging procedures has been the subject of many studies.

Imaging HER1

Several imaging modalities can be applied to detect cell surface receptor expression *in vivo*, including magnetic resonance imaging (MRI), single photon emission tomography (SPECT), positron emission tomography (PET), near-infrared (NIR) fluorescence and ultrasound. Molecular imaging requires the administration of a targeted tracer which homes in on the molecule of interest. The targeting moiety of the tracer which interacts specifically with the antigen of interest can be an antibody such as cetuximab. Attached to the targeting component is a beacon, the nature of which depends on the imaging modality employed. In the case of PET, emitted positrons interact with an electron and annihilate within a few millimetres of the decaying nucleus, producing two almost antiparallel gamma rays. These are detected by the PET camera, which consists of a ring of detectors located around the patient. Commonly for PET tracers such as antibodies, these include positron-emitting nuclides of metals such as ⁶⁴Cu ($t_{1/2}$ [half-life]=12.8 h) or ⁸⁹Zr ($t_{1/2}$ =78.4 h). Single photon emission tomography is a nuclear medicine imaging technique that can provide three-dimensional (3D) images by detection of gamma rays emitted from a targeting moiety labelled with a gamma-emitting nuclide, and SPECT tracers are commonly labelled with ^{99m}Tc ($t_{1/2}$ =6 h) or ¹¹¹In ($t_{1/2}$ =2.8 d). Metal nuclides are attached via a chelator such as diethylenetriaminepentaacetic acid (DTPA) to the targeting moiety. Labels for magnetic imaging probes are paramagnetic in nature, causing localised perturbations in water proton relaxation parameters.

Antibody-based HER1-targeting tracers

Milenic *et al.*¹⁰ produced the SPECT tracer [¹¹¹In]-CHX-A-DTPA-cetuximab and examined its binding to xenografts derived from tumour cells from several tumour types – DU-145 (prostate), LS174T (colon), HT-29 (colon), SKOV-3 (ovary), SHAW (pancreas) and A375 (melanoma) – expressing a range of HER1 levels. The correlation between [¹¹¹In]-CHX-A-DTPA-cetuximab binding and tumour cell expression of HER1 determined *in vitro* was poor. The highest uptake was

exhibited by HT-29 cells which express HER1 only at intermediate levels and have been shown to be non-responsive to cetuximab treatment.¹¹ They concluded from this that the use of radiolabelled cetuximab may be an appropriate therapy agent in cetuximab-resistant tumours which express HER1.

Barrett *et al.*¹² used ¹¹¹In to label cetuximab and also the HER2 targeting antibody trastuzumab (Herceptin). The two antibodies were also labelled with different coloured fluorescent tags which could be detected using NIR imaging. Single photon emission tomography imaging detected tumours expressing HER1 and HER2 in mice which had been implanted in opposite flanks. However, using NIR imaging, discrimination between HER1- and HER2-expressing tumours could be achieved *in vivo*. Although fluorescence imaging is restricted to superficial tissues, NIR wavelengths (650–900 nm) are not absorbed efficiently by haemoglobin, fat and muscle so are quite deeply penetrating.

The nuclear decay characteristics of ⁶⁴Cu ($t_{1/2}$ =12.7 h), including the relatively low energy (<0.7 MeV) of its emitted positrons (β^+), make it an excellent PET nuclide with respect to image quality. Eiblmaier *et al.*¹³ demonstrated that binding of the DOTA-cetuximab conjugate labelled with ⁶⁴Cu to five cervical cancer cell lines corresponded with *HER1* gene expression. Cai *et al.*¹⁴ showed that uptake of [⁶⁴Cu]-DOTA-cetuximab by xenografts derived from cancer cell lines exhibiting a broad range of HER1 expression – high: PC-3 and U87MG, medium: HCT-8 and CT-8, and low: HCT-116, SW620 and MDA-MB-453 – showed a strong correlation with HER1 protein expression determined by Western blot. Unfortunately, the application of [⁶⁴Cu]-DOTA-cetuximab to the imaging of liver metastases, commonly associated with colorectal tumours, is limited due to the high levels of liver uptake probably as a result of hepatobiliary excretion of transchelated ⁶⁴Cu.¹⁴ Despite this drawback, imaging of HER1 using [⁶⁴Cu]-DOTA-cetuximab has successfully demonstrated degradation of HER1 in the EGFR-expressing tumour cells PC3 during treatment with 17-allylamino-17-demethoxygeldanamycin (17-AAG), an inhibitor of the chaperone Hsp90, a protein that ensures the correct confirmation of several molecules including HER1, HER2 and Akt. Uptake was found to be significantly decreased by tumours in treated mice, compared with uptake by untreated tumours in untreated mice, 4 h and 24 h after injection, corresponding with decreased expression of HER1.¹⁵

The zirconium nuclide ⁸⁹Zr is a positron-emitting nuclide with a $t_{1/2}$ of about 78 h and, like ⁶⁴Cu and ⁶⁸Ga, remains within the cell's lysosomes (residualisation) after the antibody has been internalised. Aerts *et al.*¹⁶ produced desferrioximine-conjugated cetuximab to facilitate labelling with ⁸⁹Zr. The tracer was administered to mice bearing xenografts derived from A431, U-373 MG, HT-29 and T47-D tumour cell lines which express HER1 at high, medium, and low levels, respectively. Uptake of this tracer was highest in the two xenografts derived from cells expressing medium levels of HER1, and uptake in the cells with only low HER1 expression was correspondingly low. However, the high HER1 expressing A-431 cells only exhibited modest uptake of [⁸⁹Zr]-cetuximab with tumour to blood ratio not exceeding 1.5:1, suggesting that the microenvironment within some tumour types may influence

the ability of relatively large molecules like cetuximab to reach their targets.

Antibodies to HER1 have been labelled with the iodine nuclides. The LA22 anti-HER1 monoclonal antibody was labelled with ^{125}I by Zhao *et al.*¹⁷ and demonstrated specific HER1 binding to HT-29 human colonic cancer cells with a KD of 3 nM. ^{124}I is a positron-emitting nuclide with a $t_{1/2}$ of 4.2 days so it is commonly used to label whole antibodies by attachment to tyrosine residues. However, internalisation of iodine-labelled antibodies results in dehalogenation and loss of ^{124}I from the tissue. To improve the stability of the iodinated anti-HER1 antibody, the ^{124}I was first incorporated into the peptide IMP-R4,¹⁸ which was then conjugated to the antibody. When tested in mice bearing HER1-expressing xenografts, the tumour to blood ratio increased with time, reaching 5:1 by 120 h post-injection of ^{124}I -labelled anti-HER1 antibody.

Other nuclides used to label cetuximab include ^{86}Y ,¹⁹ using the bifunctional chelate CHX-A'-DTPA. The tracer exhibited good tumour uptake by HER1-expressing tumours and relatively low liver uptake. However, the energy of the β^+ emitted by ^{86}Y is high (3.1 MeV), contributing to poor image quality.

Anti-HER1 nanobody- and affibody-based tracers for HER1 imaging

Patient scanning is carried out a sufficient interval after tracer administration to allow tracer that has not become associated with its target to be cleared from the blood. The long blood residency times of whole antibodies precludes their labelling with relatively short-lived radioisotopes such as ^{68}Ga , as the time required for clearance is far longer than the $t_{1/2}$ of the nuclide. The use of a cetuximab fragment consisting of a single chain variable region with a molecular weight of less than 30 kDa has been radiolabelled but the receptor affinity for the fragment was five-fold lower than for the whole molecule.²⁰ The endogenous HER1 ligand hEGF has a molecular weight of only 6.2 kDa and exhibits rapid renal clearance so can be labelled with short-lived isotopes such as ^{68}Ga ($t_{1/2}$ =68 min), achieved using the chelating group DOTA. ^{68}Ga has the advantage that it can be produced from a $^{68}\text{Ge}/^{68}\text{Ga}$ generator which is commercially available, enabling its application at PET facilities that do not have a cyclotron. Uptake of the tracer by A431 carcinoma cells and by U343 glioma cells has been demonstrated. Uptake by A431 xenografts achieved a tumour uptake of 2.7% ID/g with a tumour to blood ratio of 4.5 after 30 min. HER1 is highly expressed by the liver and, in common with other HER1 ligands, very high liver (>30% ID/g) and kidney (>40% ID/g) uptake was demonstrated.²¹

Recently, a number of small HER1-targeting molecules have been developed and radiolabelled for HER1 imaging, including nanobodies^{22,23} and affibodies.^{24,25} Nanobodies are antigen-binding fragments from immunoglobulins found in the serum of *Camelidae* species whose immunoglobulins comprise only heavy chains.²² These fragments are approximately 15 kDa in size. Affibodies are affinity proteins consisting of 58 amino acids. They exhibit high affinity for their target molecules and, due to their small size (6.5 kDa), are cleared rapidly by the kidney. Anti-HER1 affibodies have the same binding site on the HER1 as EGF and cetuximab and are internalised after binding.²⁴

Affibodies have been labeled with ^{111}In and ^{125}I for SPECT

imaging,^{26,27} ^{64}Cu for PET imaging,²⁵ and with fluorescent probes^{28,29} for detection using a fluorescence imager.

Colorectal tumours commonly metastasise to the liver. However, the high liver uptake of HER1-targeting molecules will obscure uptake by such metastasis. To overcome the uptake by non-tumour liver tissue, a number of studies have tried co-administration of radiotracers with unlabelled tracer. Kareem *et al.*²⁷ showed that administration of cold EGF or anti-HER1 affibody with the radiolabelled EGF or anti-HER1 improved the tumour to liver ratio of radiolabelled EGF by blocking its uptake by the liver. Thus, intraperitoneal injection of non-radiolabelled EGF before intravenous injection of [^{125}I]- or [^{111}In]-labelled EGF or anti-HER1 affibody molecule $Z_{(\text{EGFR:955})2}$ administered 30 min before ^{111}In -EGF significantly decreased [^{125}I]-EGF uptake by the liver, thereby increasing the tumour to liver ratio.

Nordberg *et al.*²⁴ also compared the uptake and retention of ^{125}I - and ^{111}In -labelled versions of the dimeric affibody $Z_{(\text{EGFR:955})2}$ by A431 xenografts. More ^{111}In than ^{125}I was retained by A431 cells as metals tend to become trapped by lysosomes, whereas halogens can be released after internalisation of the HER1/HER1-targeting complex. *In vivo* uptake by A431 xenografts reached 3.8% at 4 h. A tumour/blood ratio of 9.1 was achieved within 24 h, which compared favourably with the natural ligand EGF (3.0) and the whole antibody (1.5). High uptake of ^{111}In was found in the kidney due to renal excretion and reabsorption of small proteins. This could not be inhibited by cold $Z_{(\text{EGFR:955})2}$. However, high uptake by the liver could be inhibited by cold $Z_{(\text{EGFR:955})2}$. Similarly, affibody uptake by xenografts formed from A431 cells labelled with [^{64}Cu]-DOTA-Z(EGFR:1907) showed improved tumour to liver ratio by inclusion of 50 μg cold affibody with the radiolabelled [^{64}Cu]-DOTA-Z(EGFR:1907) (5 μg).²⁵ The [^{64}Cu]-DOTA- $Z_{(\text{EGFR:1907})}$ was found to be resistant to transchelation by serum constituents.²⁵

Gong *et al.*²⁸ labelled anti-HER1 affibodies with NIR fluorophores and were able to detect xenografts derived from HER1-overexpressing A431 tumour cells *in vivo* using a fluorescence imager from 1 h post-injection. Gostring *et al.*²⁹ conjugated the HER1 targeting molecules EGF, cetuximab and the EGFR-binding affibody $Z_{(\text{EGFR:1907})}$ with the fluorescent marker Alexa488 and measured the rate of internalisation using an Alexa488-quenching method in which the fluorescence from Alexa488 is measured in the presence and absence of anti-Alexa488 antibody, which quenches fluorescence from extracellular Alexa488-labelled molecules. Using this method 45% of EGF and cetuximab, and about 20% of the affibody were found to be internalised within 1 h. These findings were corroborated using ligands labelled with ^{111}In using an acid wash procedure to remove non-internalised ligand. The fluorescence quenching technique has the advantage that not all ligands that include the anti-HER1 affibody are susceptible to the acid hydrolysis procedure.

Receptor internalisation can be exploited for the cellular delivery of molecular conjugates. A novel bispecific immunoconjugate, [^{111}In]-labelled EGF-anti-p27^{KIP1} consisting of EGF conjugated with anti-p27^{KIP1}, ^{111}In -DTPA and a nuclear localising sequence, was synthesised by Cornelissen *et al.*³⁰ The EGF component facilitates binding to HER1 and internalisation of the molecule. The anti-p27^{KIP1} component binds to the downstream cyclin-dependent kinase 1, p27^{KIP1}, to probe its expression by cells during treatment with anti-HER2 therapy.³⁰

Tyrosine kinase inhibitors

A number of tyrosine kinase inhibitors have been developed as anticancer agents targeting the active site on the intracellular component of HER receptors. Positron emission tomography tracers based on ^{18}F and ^{124}I versions of some of these agents have been produced, but their performance as imaging agents has proved disappointing. Su *et al.*³¹ synthesised ^{18}F -labelled gefitinib and determined its uptake *in vitro* and *in vivo* by U87 cells which express low levels of HER1, and in U87-EGFR cells in which the HER1 had been transfected. They also examined the effect of HER1 kinase mutations on [^{18}F]-gefitinib uptake by two human non-small cell lung carcinoma (NSCLC) cell lines, H3255 and H1975. Both express a point mutation (L858R) which confers high sensitivity to gefitinib, but H1975 also carries a further mutation that makes it resistant to gefitinib. In tumour-bearing mice, the lipophilic [^{18}F]-gefitinib exhibited rapid hepatobiliary excretion with uptake by the liver dominating the images. There was little difference in uptake between tumours *in vivo*, which was attributed to a high degree of non-specific binding of [^{18}F]-gefitinib (due to the lipophilicity of gefitinib, possibly resulting in non-targeted binding in cell membranes), as incubation of cells with non-labelled gefitinib only decreased binding of labelled gefitinib by one of the cell lines.

In contrast to gefitinib, ML04, a derivative of the 4-dimethylamino-but-2-enoic acid (4-[phenylamino]-quinazoline-6-yl)-amide group, is an irreversible tyrosine kinase inhibitor, as sustained inhibition of HER1 phosphorylation occurs even after removal of ML04 from the growth medium. However, as with [^{18}F]-gefitinib, [^{18}F]-ML04 exhibited predominantly non-specific binding when imaged in mice bearing HER1-overexpressing xenografts.³²

More encouraging results have been achieved³³ using morpholino- [^{124}I]-IPQA ([E]-But-2-enedioic acid [4-(3-[^{124}I]iodoanilino)-quinazolin-6-yl]-amide-[3-morpholin-4-yl-propyl]-amide) that selectively, irreversibly and covalently binds to the activated (phosphorylated) HER1 kinase, but not to the inactive (non-phosphorylated) HER1 kinase. A431, an NSCLC tumour cell line which overexpresses HER1, a U87 cell line in which mutant HER1 had been transfected which expresses a high level of active phosphorylated HER1, and U87 wild-type cells were incubated with this molecule and uptake and washout measured during serum starvation (to deactivate HER1). Rapid uptake by all three tumours was observed but the two cell lines overexpressing HER1 retained higher levels of activity than did the U87 wild-type cells. Uptake by xenografts derived from A431 was three times higher than by xenografts derived from K562 cells grown in either rats or mice which do not overexpress HER1.

Effect of mutations in effectors downstream of HER1 on response to anti-HER1

Although tumour HER1 expression can be a useful indicator for treatment with anti-HER1 therapies, factors downstream of HER1 will modulate the therapeutic efficacy of such treatments.^{34,35} Mutated *K-ras* is associated with a state of pathway activation and resistance to cetuximab treatment. Other factors downstream of the HER1 pathway are also associated with resistance to cetuximab.³⁶ In a study⁴ of 78 lung cancer patients treated with gefitinib, six tumours had

K-ras mutations and did not respond to gefitinib, two patients with PIK3CA showed partial response, but in patients with *HER1* mutations survival was longest in those with high PIK3CA or PTEN expression. Personeni *et al.*⁷ also showed that the potentially beneficial role of high HER1 expression in colorectal cancer patients treated with cetuximab was counteracted by the presence of *K-ras* mutations.

Use of [^{18}F]-FDG to measure response to anti-HER1 treatment

Changes in the activation of the Akt pathway have been shown to cause increased glucose metabolism, while disruption of the PI3/Akt pathway by inhibition of PI3K results in decreased glucose consumption.³⁷ Park *et al.*³⁸ have shown, in a retrospective study of 53 patients with lung adenocarcinomas, that high [^{18}F]-FDG incorporation was associated with increased *HER1* gene copy number. Huang *et al.*³⁹ have recently shown, in a study of 77 patients with advanced stage IIIB or IV lung adenocarcinoma in whom [^{18}F]-FDG PET and *HER1* mutation analysis was carried out on treatment-naïve patients, that [^{18}F]-FDG uptake was significantly higher in *HER1*-mutant (10.5±4.7) compared to wild-type (8.0±3.3) lung adenocarcinoma patients.

CI-1033 is a quinazoline-based irreversible inhibitor that acts by alkylating a cysteine in the kinase domain of HER proteins, blocking catalytic activity and downstream signalling. Dorow *et al.*⁴⁰ examined the effect of treating A431 xenografts with CI-1033 on uptake of [^{18}F]-FDG, [^{18}F]-FLT and the tumour hypoxia marker [^{18}F]-FAZA. Uptake was measured in untreated and treated tumours. All three tracers exhibited significant decreases in uptake after six or seven days of treatment. Changes in [^{18}F]-FDG uptake correlated with decreased glut-1 expression by CI-1033-treated tumours compared with controls, while [^{18}F]-FLT, a tracer phosphorylated by thymidine kinase, correlated with changes in BrdU incorporation, a measure of DNA synthesis, on day 6 of treatment.

In this study, we investigate the association between [^{18}F]-FDG incorporation and breast cancer response to the anti-HER1 antibody cetuximab in the breast tumour cell line MDA-MB-468, which shows high-level *HER1* expression, and in two cell lines (SKBr-3 and MDA-MB-453) that express *HER1* at low levels. Growth inhibition is determined using an MTT assay and verified using a clonogenic assay. Glucose transport and hexokinase activity, which influence [^{18}F]-FDG incorporation and are sensitive to changes in the activity of the PI3K/Akt intracellular pathways, are also determined.

Materials and methods

All chemicals were obtained from Sigma-Aldrich (Poole, UK) unless otherwise stated. Cell lines were obtained from the American Type Culture Collection (ATCC) (Manassas, Virginia, USA).

Cells and treatments

SKBr3, MDA-MB-453 and MDA-MB-468 cells were cultured in DMEM (Invitrogen, Paisley, UK), supplemented with 50 units/mL penicillin, 50 µg/mL streptomycin and 10% fetal bovine serum (FBS) for maintenance and 2% FBS during drug incubations.

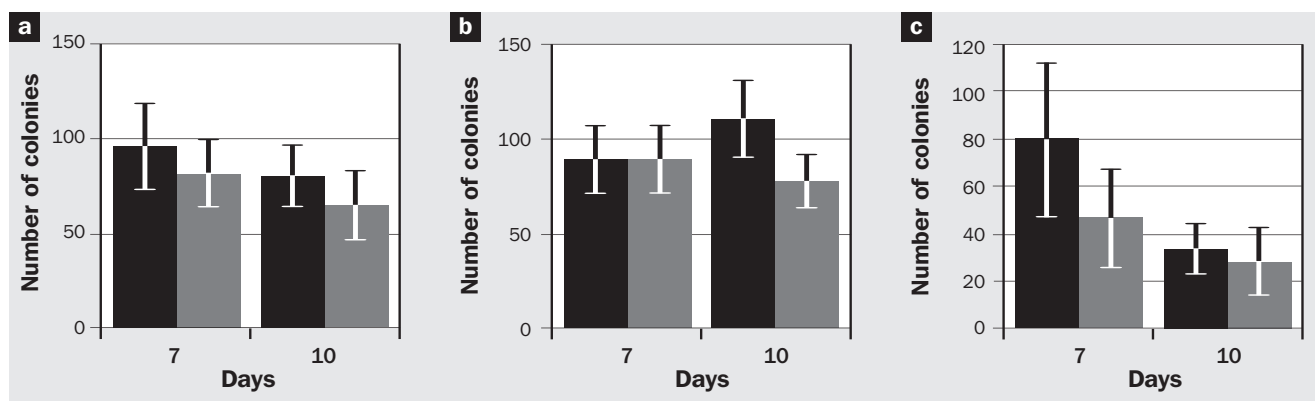


Fig. 1. Formation of colonies of >25 (day 7) or >50 (day 10) cells by SKBr3 (a), MDA-MB-453 (b) or MDA-MB-468 (c) breast tumour cells treated with low (black) (IC_5 for SKBr3 and MDA-MB-453 or IC_{20} for MDA-MB-468) and with high (grey) (IC_{10} for SKBr3 and MDA-MB-453, IC_{50} for MDA-MB-468) doses of cetuximab.

MTT assay

Cell suspensions (100 μ L; 1500 SKBr3 cells and MDA-MB-453 cells, 750 MDA-MB-468 cells) were seeded in 96-well plates and incubated at 37°C overnight. Medium (100 μ L) containing cetuximab (final concentrations SKBr3: 0.1–250 μ g/mL; MDA-MB-453: 0.1–250 μ g/mL; MDA-MB-468: 0.01–10 μ g/mL) was added to each well (200 μ L/well) and the plate returned to the incubator. A background of 200 μ L medium and a control of 200 μ L medium and cells were also prepared. After six days, 50 μ L MTT was added to each well and incubated for 3–4 h. The medium was then aspirated and replaced with 200 μ L dimethyl sulphoxide (DMSO). The plate was then read at 570 nm in a scanning multiwell spectrophotometer (Dynatech MR5000, Dynatech Laboratories Chantilly, VA, USA) after a 30-sec agitation (test filter: 570 nm, reference filter: 690 nm) and the readings analysed using Biolinx 2.0 software (Biolinx 2.0, Dynatech Laboratories).

Colony formation

The ability of SKBr3 and MDA-MB-453 cells treated continuously with cetuximab (IC_5 and IC_{10}) and MDA-MB-468 cells (IC_{20} and IC_{50}) to proliferate was determined by seeding cells in 25 cm^2 tissue culture flasks (20,000 per flask in triplicate per treatment) and assessing the number of cells that formed colonies of at least 25 cells after seven days and at least 50 cells by day 10 (results expressed relative to control flasks). Colony counts were carried out using a Nikon Eclipse TS100 inverted microscope with a 10x objective lens, counting cells in 20 fields per flask.

FDG incorporation

Cells were seeded in 25 cm^2 tissue culture flasks for three days then treated with doses of cetuximab for 4 h, two, four and six days. The medium was replaced with 1 mL fresh medium (glucose concentration: 1 mg/mL [5 mmol/L]) containing 37 KBq [^{18}F]FDG and incubated for 20 min at 37°C. Cells were then washed (x5) with 5 mL ice-cold phosphate-buffered saline (PBS), detached by the addition of trypsin, and neutralised with medium. Activity in the cell suspension was determined in a well counter. The cells were then centrifuged, washed with 1 mL PBS, the pellet dissolved in 0.1 mL NaOH (1 mol/L) and neutralised with 0.1 mL HCl. Protein content was determined using a bicinchoninic acid (BCA) protein assay kit (Sigma, Poole, UK).

Glucose transport

Glucose transport rate was determined by measuring the rate of incubation of [3H] o-methyl-glucose ([3H] OMG) before equilibrium occurred. Flasks of cells were set up and treated for six days (as above). At the time of glucose transport determination, the medium was removed and replaced with fresh medium (glucose concentration 1 mg/mL to simulate blood glucose level) containing 37 KBq [3H] OMG and 0.1 mmol/L 'cold' OMG for 5 sec. Four rapid washes, each using 5 mL ice-cold PBS containing the glucose transport inhibitor phloretin (0.1 mmol/L), were carried out and cells were detached using 0.5 mL trypsin, then neutralised with medium. Cell suspension (0.5 mL) was added to 5 mL Optima Gold scintillation fluid (Perkin Elmer, UK) and [3H] OMG uptake was determined in a scintillation counter. The remaining cells were prepared for the protein assay (as for FDG).

Hexokinase activity

Cells were seeded in 25 cm^2 flasks, treated with cetuximab for six days then detached with trypsin. After addition of medium, they were collected into microfuge (Eppendorf) tubes, washed with PBS, centrifuged at 400 xg for 1 min and the pellet resuspended in 0.2 mL homogenisation buffer (10 mmol/L Tris/HCl [pH 7.7], 0.25 mmol/L sucrose, 0.5 mmol/L dithiothreitol, 1 mmol/L aminohexanoic acid, 1 mmol/L phenylmethylsulphonyl fluoride [PMSF]). The suspension was then transferred to a 1 mL glass Douce homogeniser and homogenised using 10 strokes at 4°C. The homogenised cells were transferred to a microfuge tube and centrifuged for 10 min at 800 xg to remove cell debris. The supernatant was transferred to a new microfuge tube and the pellet was washed with 0.2 mL homogenisation buffer and the

Table 1. Growth inhibitory doses (μ g/mL) for breast tumour cells treated with cetuximab for six days determined using the MTT assay.

| | SKBr3 | MDA-MB-453 | MDA-MB-468 |
|-----------|-------|------------|------------|
| IC_{50} | – | – | 2.6 |
| IC_{20} | – | – | 0.63 |
| IC_{10} | 5 | 148 | – |
| IC_5 | 0.8 | 0.6 | – |

supernatant pooled. Protein content of the homogenate was determined using a 20 μ L sample.

Enzyme activity was determined by addition of 100 μ L homogenate to 0.9 mL assay medium consisting of 100 mmol/L Tris/HCl (pH 8.0), 10 mmol/L glucose, 0.4 mmol/L NADP⁺, 10 mmol/L MgCl₂, 5 mmol/L ATP and 0.15 units glucose-6-phosphate dehydrogenase in a cuvette at 37°C. The reaction was followed by monitoring the change in absorbance at 340 nm due to the formation of NADPH.

Lactate production

Cells were prepared and treated for six days as for glucose uptake determination. The cells were then washed (x4) with PBS and incubated for 30 min with Dulbecco's modified Eagle's medium (DMEM) containing 1 mg/mL glucose. The medium was then removed and stored at -20°C until lactate was assayed. Cells were then trypsinised and prepared for protein assay as for FDG incorporation. Lactate was assayed in the medium using a lactate assay kit (BioVision, California, USA), following the manufacturer's instructions.

Statistics

Significant differences between means were established using Student's *t*-test. Values are included in the text and include the number of degrees of freedom (=total number of replicates in control and treatment group -2).

Results

Inhibitory doses for cetuximab incubated for six days with MDA468, MDA453 and SKBr3 breast tumour cells are shown in Table 1. Inhibition of SKBr3 and MDA-MB-453 cells with cetuximab reached a plateau at 10% (5 μ g/mL and 148 μ g/mL doses, respectively). Further growth inhibition could not be achieved using higher doses. MDA-MB-468 cells were very sensitive to treatment with cetuximab and 50% inhibition was achieved with a dose of 2.6 μ g/mL.

Figure 1 shows the effect of growth inhibitory doses of cetuximab on the clonogenic potential of each cell line after seven and 10 days of continuous exposure to each drug dose. Continuous exposure of MDA-MB-468 cells to IC₂₀ and IC₅₀ doses of cetuximab by 10 days had decreased colony forming ability to approximately 30%.

Results of the incorporation of FDG (per mg protein) relative to untreated controls after treatment of SKBr3 and MDA-MB-453 cells with IC₅ and IC₁₀ and MDA-MB468 cells with IC₂₀ and IC₅₀ doses of cetuximab for 4 h, two, four and six days relative to untreated cells are shown in Figure 2. FDG incorporation by SKBr3 cells was not significantly changed by treatment with IC₅ or IC₁₀ doses of cetuximab for 4 h ($t_6=0.94$ ns, $t_6=1.12$, respectively), two days ($t_{25}=0.96$ ns, $t_{24}=0.5$ ns, respectively), four days ($t_{14}=0.25$ ns, $t_{14}=0.31$, respectively) or six days ($t_{20}=1$ ns, $t_{21}=0.45$ ns, respectively). MDA-MB-453 cells exhibited decreased FDG incorporation after six days of treatments with IC₅ and IC₁₀ doses of cetuximab ($t_{13}=2.62$ [$P<0.005$], $t_{13}=3.24$ [$P<0.005$], respectively) but not 4 h ($t_{14}=0.23$ ns, $t_{14}=1.04$ ns, respectively), two days ($t_{13}=1.16$ ns, $t_{12}=0.41$ ns, respectively) or four days ($t_6=0.14$ ns, $t_6=0.82$ ns, respectively) of treatment. FDG incorporation was significantly decreased by MDA-MB-468 cells after treatment with IC₂₀ and IC₅₀ doses of cetuximab for 4 h ($t_{35}=5.18$ [$P<0.001$], $t_{22}=3.66$ [$P<0.01$], respectively), two days

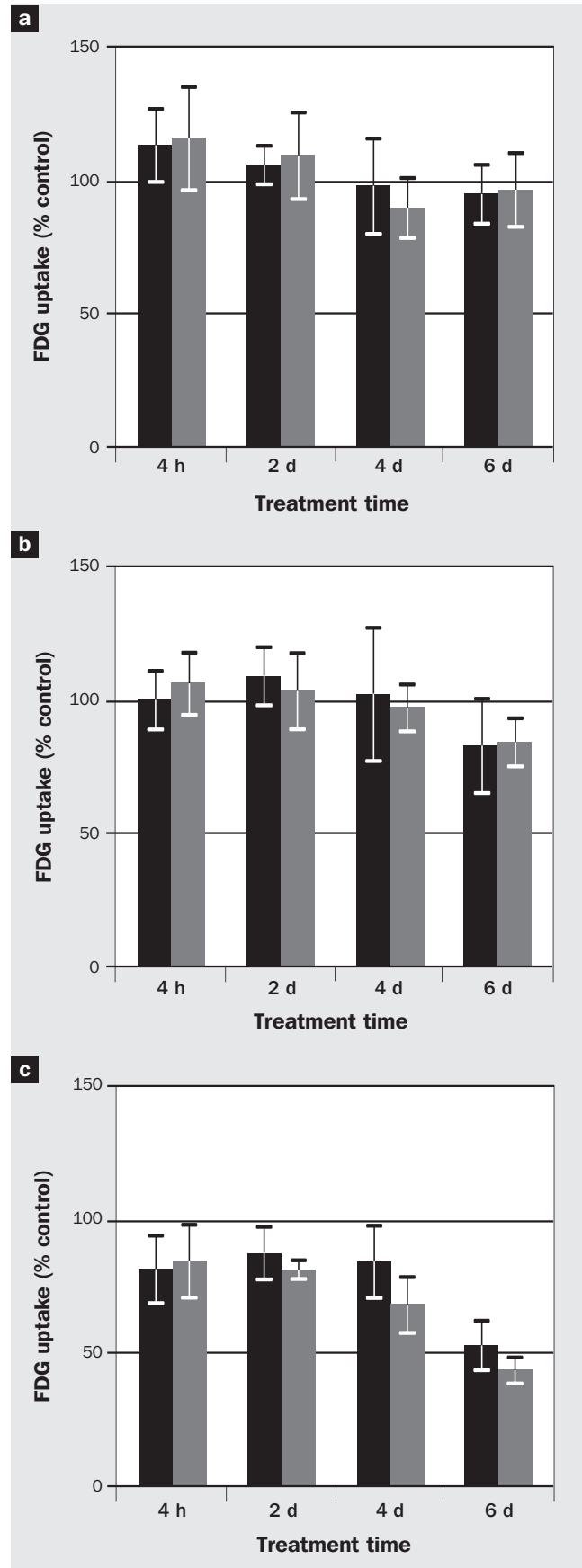


Fig. 2. FDG incorporation per mg protein after cetuximab treatment of SKBr3 (IC₅ [black] and IC₁₀ [grey]) (a), MDA-MB-453 (IC₅ [black] and IC₁₀ [grey]) (b) and MDA-MB-468 (IC₂₀ [black] and IC₅₀ [grey]) (c).

($t_6=1.73$, $t_6=4.19$ [$P<0.005$] respectively), four days ($t_{12}=2.67$ [$P<0.05$], $t_{12}=3.26$ [$P<0.005$], respectively) and six days ($t_{12}=11.45$ [$P<0.001$], $t_{12}=18.1$ [$P<0.001$], respectively).

Hexokinase (HK) activity in homogenates prepared from SKBr3, MDA-MB-453 and MDA-MB-468 cells treated with cetuximab for six days is shown in Figure 3A as a percentage of the activity in respective untreated cells. Activity was decreased by cetuximab in MDA-MB-468 cells ($t_{21}=3.31$ [$P<0.005$]) compared with controls but not in SKBr3 ($t_{14}=0.92$ ns) or MDA-MB-453 ($t_{12}=1.39$ ns) cells.

Figure 3B shows the uptake of [^3H]-o-methylglucose (OMG) by untreated cells incubated with [^3H]-OMG (0.1 mmol/L OMG) for 5 sec and by cells treated with cetuximab. Cetuximab treatment for six days did not significantly change glucose transport in SKBr3 ($t_6=0.65$ ns), MDA-MB-453 ($t_{15}=0.22$ ns) or MDA-MB-468 ($t_6=1.55$ ns) cells.

Lactate production was measured in each cell line after treatment for six days with cetuximab. The results in Figure 4 show that response to cetuximab treatment does not result in a decrease in lactate production in SKBr3 ($t_6=1.11$ ns) or MDA-MB-453 ($t_{12}=0.64$ ns) cells, and increases production by MDA-MB-468 cells ($t_{12}=3.04$ [$P<0.001$]).

Discussion

Studies have shown that tumour expression of HER1 does not correspond with response to cetuximab.⁴¹⁻⁴⁴ In a study of 20 patients with metastatic colorectal cancer, Habbar *et al.*⁴³ showed an objective response to cetuximab by four patients, all of whom had HER1-negative tumours. In a multicentre trial of 346 patients⁴⁴ with colorectal cancer treated with cetuximab, clinical benefit in terms of best response to cetuximab, progression-free survival or overall survival did not relate to HER1 immunostaining, the presence of HER1 tyrosine kinase domain mutations or to *HER1* gene copy number. In the present study, cetuximab was found to have a slight growth inhibitory effect, determined by MTT assay and clonogenic survival, on breast tumour cells that did not overexpress HER1.

The MTT assay depends on the reduction of tetrazolium dye by mitochondrial enzymes as a measure of viable cell number. To ensure that this is a true representation of the ability of cetuximab to inhibit long-term proliferative ability, colony formation assays were also carried out to measure the ability of cetuximab to induce clonogenic cell death.^{45,46} Taken together, the results of the MTT and clonogenic assays suggest that cetuximab does have limited antiproliferative activity against the two breast tumour cells lines (SKBr3, MDA-MB-435) that do not overexpress HER1. In contrast, the HER1-overexpressing cell line MDA-MB-468 was found to be very sensitive to cetuximab. The MTT assay appeared to underestimate the antiproliferative effect of cetuximab when compared with the 10-day clonogenic assay. This concurs with previous findings of the treatment effect of chemotherapy agents such as oxaliplatin, irinotecan⁷ and cisplatin.⁴⁶

Cells that were highly sensitive to cetuximab (i.e., MDA-MB-468) exhibited decreased FDG incorporation relative to untreated cells when treated with IC_{50} doses of cetuximab for four and six days, and when treated with IC_{20} doses of cetuximab for six days. FDG incorporation by MDA-MB-453

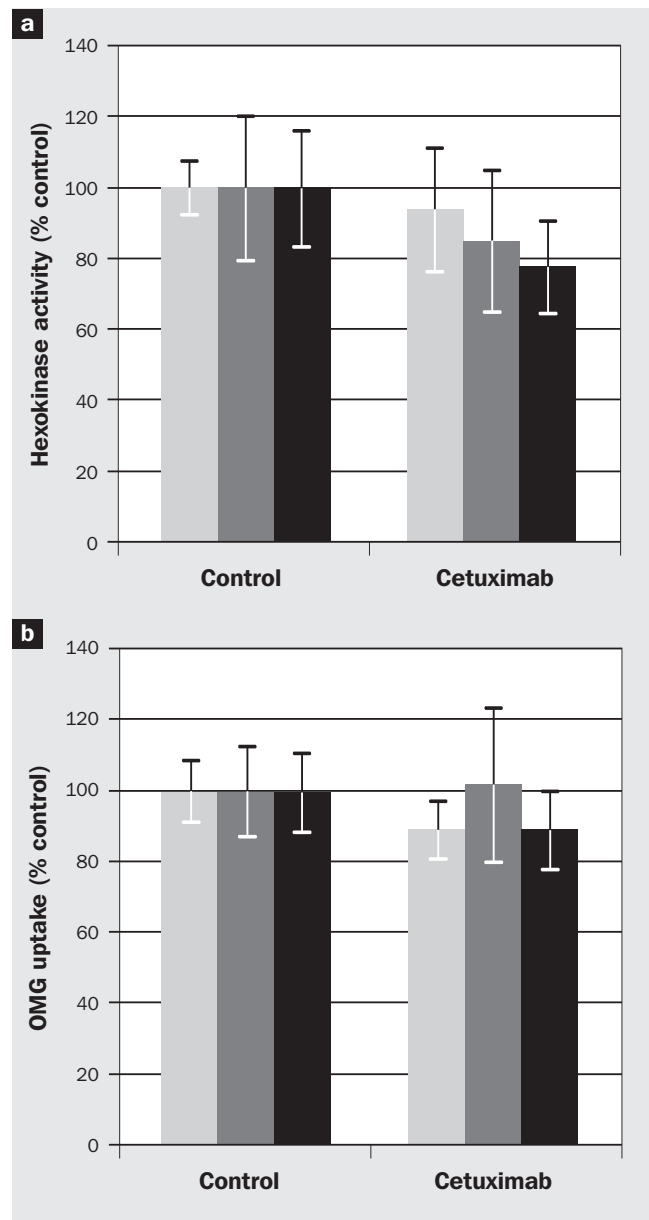


Fig. 3. Hexokinase activity (a) and glucose transport (b) by SKBr3 (light grey), MDA-MB-453 (dark grey) and MDA-MB-468 (black) cells treated with IC_{10} , IC_{10} and IC_{50} doses of cetuximab.

cells treated with cetuximab that produced only a marginal growth-inhibitory effect exhibited only a slight decrease in FDG incorporation after six days of treatment.

Glucose transport and HK are involved in the cellular incorporation of FDG and the rate-limiting step for tumour FDG incorporation varies with tumour type. An *in vivo* study has shown that, in breast cancers, HK activity is rate limiting.⁴⁷ The present study found that HK activity, but not glucose transport, was inhibited in MDA-MB-468 cells responding to treatment with cetuximab. Correspondingly, HK activity has also been shown to be increased in cells incubated with ligand activators of HER1.⁴⁸ A decrease in HK activity by MDA-MB-453 cells was not detected, despite a small decrease in FDG incorporation. However, HK activity was determined on cell lysates and therefore small changes in HK activity may be difficult to detect in disrupted cells.

Incorporation of FDG measures the rate of glucose

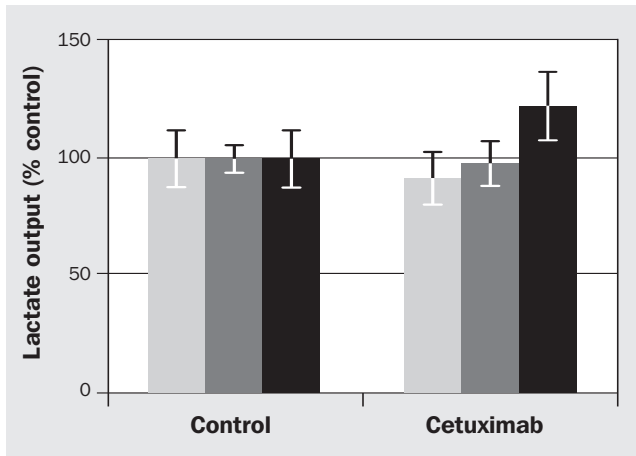


Fig. 4. Lactate production by SKBr3 (light grey), MDA-MB-453 (dark grey) and MDA-MB-468 (black) cells treated with IC_{10} , IC_{20} and IC_{50} doses of cetuximab.

utilisation via glycolysis. The product of glycolysis, pyruvate, can either be converted to acetyl-CoA and enter the tricarboxylic acid cycle or be converted to lactic acid. A number of other fuel sources, including glutamine, can also be converted to lactic acid.⁴⁹ Decreased lactate levels in tumours during therapy, compared with pretreatment levels, have been shown to be a useful indicator of response to therapy.⁵⁰ However, treatment of MDA-MB-468 cells with cetuximab, which was associated with decreased FDG incorporation, did not result in decreased lactate production, which suggests that monitoring tumour lactate levels is not useful for predicting response to cetuximab. As pyruvate production from glucose via glycolysis is not the only source of lactate in tumour cells, the absence of a correlation between lactate production and FDG utilisation is not unexpected.

In conclusion, treatment of breast tumour cells that overexpress HER1 with growth inhibitory doses of cetuximab results in decreased FDG incorporation at the tumour cell level.

Funding by the Breast Cancer Campaign (Grant No. 2006PhdNov02) is gratefully acknowledged.

References

- Klijn JG, Berns PM, Schmitz PI, Foekens JA. The clinical significance of epidermal growth factor receptor (EGFR) in human breast cancer: a review on 5232 patients. *Endocr Rev* 1991; **13**: 3–17.
- Zhang Y, Opresko L, Shankaran H, Chrisler WB, Wiley HS, Resat H. HER/ErbB receptor interactions and signaling patterns in human mammary epithelial cells. *BMC Cell Biol* 2009; **10**: 78.
- Messersmith W, Oppenheimer D, Peralba J *et al.* Assessment of epidermal growth factor receptor (EGFR) signaling in paired colorectal cancer and normal colon tissue samples using computer-aided immunohistochemical analysis. *Cancer Biol Ther* 2005; **4**: 1381–6.
- Endoh H, Yatabe Y, Kosaka T, Kuwano H, Mitsudomi T. PTEN and PIK3CA expression is associated with prolonged survival after gefitinib treatment in EGFR-mutated lung cancer patients. *J Thorac Oncol* 2006; **1**: 629–34.
- Jain A, Penuel E, Mink S *et al.* HER kinase axis receptor dimer partner switching occurs in response to EGFR tyrosine kinase inhibition despite failure to block cellular proliferation. *Cancer Res* 2010; **70**: 1989–99.
- Perez-Torres M, Guix M, Gonzalez A, Arteaga CL. Epidermal growth factor receptor (EGFR) antibody down-regulates mutant receptors and inhibits tumors expressing EGFR mutations. *J Biol Chem* 2006; **281**: 40183–92.
- Personeni N, Fieuws S, Piessevaux H *et al.* Clinical usefulness of EGFR gene copy number as a predictive marker in colorectal cancer patients treated with cetuximab: a fluorescent *in situ* hybridization study. *Clin Cancer Res* 2008; **14**: 5869–76.
- Scartozzi M, Bearzi I, Berardi R *et al.* Epidermal growth factor receptor (EGFR) status in primary colorectal tumors does not correlate with EGFR expression in related metastatic sites: implications for treatment with EGFR-targeted monoclonal antibodies. *J Clin Oncol* 2004; **22**: 4772–8.
- Italiano A, Vandebos FB, Otto J *et al.* Comparison of the epidermal growth factor receptor gene and protein in primary non-small cell lung cancer and metastatic sites: implications for treatment with EGFR inhibitors. *Ann Oncol* 2006; **17**: 981–5.
- Milenic DE, Wong KJ, Baidoo KE *et al.* Cetuximab: preclinical evaluation of a monoclonal antibody targeting EGFR for radioimmunodiagnostic and radioimmunotherapeutic applications. *Cancer Biother Radiopharmaceut* 2008; **23**: 619–31.
- Wild R, Fager K, Flefle C *et al.* Cetuximab preclinical antitumor activity (monotherapy and combination based) is not predicted by relative total or activated epidermal growth factor receptor tumor expression levels. *Mol Cancer Ther* 2006; **5**: 104.
- Barrett T, Koyama Y, Hama Y *et al.* *In vivo* diagnosis of epidermal growth factor receptor expression using molecular imaging with a cocktail of optically labeled monoclonal antibodies. *Clin Cancer Res* 2007; **13**: 6639–48.
- Eiblmaier M, Meyer LA, Watson MA, Fracasso PM, Pike LJ, Anderson CJ. Correlating EGFR expression with receptor-binding properties and internalization of Cu-64-DOTA-cetuximab in 5 cervical cancer cell lines. *J Nucl Med* 2008; **49**: 1472–9.
- Cai WB, Chen K, He LN, Cao QH, Koong A, Chen XY. Quantitative PET of EGFR expression in xenograft-bearing mice using Cu-64-labeled cetuximab, a chimeric anti-EGFR monoclonal antibody. *Eur J Nucl Med Mol Imaging* 2007; **34**: 850–8.
- Niu G, Cai WB, Chen K, Chen XY. Non-invasive PET imaging of EGFR degradation induced by a heat shock protein 90 inhibitor. *Mol Imaging Biol* 2008; **10**: 99–106.
- Aerts HJWL, Dubois L, Perk L *et al.* Disparity between *in vivo* EGFR expression and Zr-89-labeled cetuximab uptake assessed with PET. *J Nucl Med* 2009; **50**: 123–31.
- Zhao HY, Jia B, Wang F, Liu ZF. Tumor targeting of I-125-labeled anti-EGFR monoclonal antibody LA22 in HT-29 human colon cancer. *Nucl Sci Techniques* 2010; **21**: 84–8.
- Lee FT, O'Keefe GJ, Gan HK *et al.* Immuno-PET quantitation of de2-7 epidermal growth factor receptor expression in glioma using I-124-IMP-R4-labeled antibody ch806. *J Nucl Med* 2010; **51**: 967–72.
- Nayak TK, Regino CAS, Wong KJ *et al.* PET imaging of HER1-expressing xenografts in mice with ⁸⁶Y-CHX-A'-DTPA-cetuximab. *Eur J Nucl Med Mol Imaging* 2010; **37**: 1368–76.
- Fan Z, Masui H, Altas I *et al.* Blockage of epidermal growth factor receptor function by bivalent and monovalent fragments of C225 anti-epidermal growth factor receptor monoclonal antibodies. *Cancer Res* 1993; **53**: 4322.

- 21 Velikyan I, Sundberg AL, Lindhe O *et al.* Preparation and evaluation of Ga-68-DOTA-hEGF for visualization of EGFR expression in malignant tumors. *J Nucl Med* 2005; **46**: 1881–8.
- 22 Gainkam LOT, Huang L, Caveliers V *et al.* Comparison of the biodistribution and tumor targeting of two Tc-99m-labeled anti-EGFR nanobodies in mice, using pinhole SPECT/micro-CT. *J Nucl Med* 2008; **49**: 788–95.
- 23 Huang L, Gainkam LOT, Caveliers V *et al.* SPECT imaging with Tc-99m-labeled EGFR-specific nanobody for *in vivo* monitoring of EGFR expression. *Mol Imaging Biol* 2008; **10**: 167–75.
- 24 Nordberg E, Friedman M, Gostring L *et al.* Cellular studies of binding, internalization and retention of a radiolabeled EGFR-binding affibody molecule. *Nucl Med Biol* 2007; **34**: 609–18.
- 25 Miao Z, Ren G, Liu HG, Jiang L, Cheng Z. Small-animal PET imaging of human epidermal growth factor receptor positive tumor with a Cu-64 labeled affibody protein. *Bioconjug Chem* 2010; **21**: 947–54.
- 26 Nordberg E, Orlova A, Friedman M, Tolmachev V, Stahl S, Nilsson FY. *In vivo* and *in vitro* uptake of In-111, delivered with the affibody molecule (Z[EGFR : 955])(2), in EGFR expressing tumour cells. *Oncol Rep* 2008; **19**: 853–7.
- 27 Kareem H, Sandstrom K, Elia R *et al.* Blocking EGFR in the liver improves the tumor-to-liver uptake ratio of radiolabeled EGF. *Tumour Biol* 2010; **31**: 79–87.
- 28 Gong HB, Kovar J, Little G, Chen HX, Olive DM. *In vivo* imaging of xenograft tumors using an epidermal growth factor receptor-specific affibody molecule labeled with a near-infrared fluorophore. *Neoplasia* 2010; **12**: 139–49.
- 29 Gostring L, Chew MT, Orlova A *et al.* Quantification of internalization of EGFR-binding affibody molecules: methodological aspects. *Int J Oncol* 2010; **36**: 757–63.
- 30 Cornelissen B, Kersemans V, McLarty K, Tran L, Reilly RM. In-111-labeled immunconjugates (ICs) bispecific for the epidermal growth factor receptor (EGFR) and cyclin-dependent kinase inhibitor, p27Kip1. *Cancer Biother Radiopharm* 2009; **24**: 163–73.
- 31 Su H, Seimille Y, Ferl GZ *et al.* Evaluation of [(18)F]gefitinib as a molecular imaging probe for the assessment of the epidermal growth factor receptor status in malignant tumors. *Eur J Nucl Med Mol Imaging* 2008; **35**: 1089–99.
- 32 Abourbeh G, Dissoki S, Jacobson O *et al.* Evaluation of radiolabeled ML04, a putative irreversible inhibitor of epidermal growth factor receptor, as a bioprobe for PET imaging of EGFR-overexpressing tumors. *Nucl Med Biol* 2007; **34**: 55–70.
- 33 Pal A, Glekas A, Doubrovin M *et al.* Molecular imaging of EGFR kinase activity in tumors with I-124-labeled small molecular tracer and positron emission tomography. *Mol Imaging Biol* 2006; **8**: 262–77.
- 34 Pantaleo MA, Nannini M, Fanti S, Boschi S, Lollini PL, Biasco G. Molecular imaging of EGFR: it's time to go beyond receptor expression. *J Nucl Med* 2009; **50**: 1195–6.
- 35 Lynch TJ, Bell DW, Sordella R *et al.* Activating mutations in the epidermal growth factor receptor underlying responsiveness of non-small cell lung cancer to gefitinib. *N Engl J Med* 2004; **350**: 2129–39.
- 36 Lièvre A, Bachet JB, Le Corre D *et al.* KRAS mutation status is predictive of response to cetuximab therapy in colorectal cancer. *Cancer Res* 2006; **66**: 3992–5.
- 37 Elstrom RL, Bauer DE, Buzzai M *et al.* Akt stimulates aerobic glycolysis in cancer cells. *Cancer Res* 2004; **64**: 3892–9.
- 38 Park EA, Lee HJ, Kim YT *et al.* EGFR gene copy number in adenocarcinoma of the lung by FISH analysis: investigation of significantly related factors on CT, FDG-PET, and histopathology. *Lung Cancer* 2009; **64**: 179–86.
- 39 Huang CT, Yen RF, Cheng MF, Hsu YC, Wei PF, Tsai YJ. Correlation of F-18 fluorodeoxyglucose-positron emission tomography maximal standardized uptake value and EGFR mutations in advanced lung adenocarcinoma. *Med Oncol* 2010; **27**: 9–15.
- 40 Dorow DS, Cullinane C, Conus N *et al.* Multi-tracer small animal PET imaging of the tumour response to the novel pan-ErbB inhibitor CI-1033. *Eur J Nucl Med Mol Imaging* 2006; **33**: 441–52.
- 41 Italiano A. Targeting the epidermal growth factor receptor in colorectal cancer: advances and controversies. *Oncology* 2006; **70**: 161–7.
- 42 Chung KY, Shia J, Kemeny NE *et al.* Cetuximab shows activity in colorectal cancer patients with tumors that do not express the epidermal growth factor by immunohistochemistry. *J Clin Oncol* 2005; **23**: 1803–10.
- 43 Hebbbar M, Wacrenier A, Desauw C *et al.* Lack of usefulness of epidermal growth factor receptor expression determination for cetuximab therapy in patients with colorectal cancer. *Anticancer Drugs* 2006; **17**: 855–7.
- 44 Lenz HJ, Van Cutsem E, Khambata-Ford S *et al.* Multicenter phase II and translational study of cetuximab in metastatic colorectal carcinoma refractory to irinotecan, oxaliplatin, and fluoropyrimidines. *J Clin Oncol* 2006; **24**: 4914–21.
- 45 Carmichael J, DeGraff WG, Gazdar AF, Minna JD, Mitchell JB. Evaluation of a tetrazolium-based semiautomated colorimetric assay: assessment of chemosensitivity testing. *Cancer Res* 1987; **47**: 936–42.
- 46 Henriksson E, Kjellen E, Wahlberg P, Wennerberg J, Kjellstrom JH. Differences in estimates of cisplatin-induced cell kill *in vitro* between colorimetric and cell count/colony assays. *In Vitro Cell Dev Biol Anim* 2006; **42**: 320–3.
- 47 Torizuka T, Zasadny KR, Recker B, Wahl RL. Untreated primary lung and breast cancers: correlation between F-18 FDG kinetic rate constants and findings of *in vitro* studies. *Radiology* 1998; **207**: 767–74.
- 48 Bryson JM, Coy PE, Gottlob K, Hay N, Robey RB. Increased hexokinase activity, of either ectopic or endogenous origin, protects renal epithelial cells against acute oxidant-induced cell death. *J Biol Chem* 2002; **277**: 11392–400.
- 49 Helmlinger G, Sckell A, Dellian M, Forbes NS, Jain RK. Acid production in glycolysis-impaired tumors provides new insights into tumor metabolism. *Clin Cancer Res* 2002; **8**: 1284–91.
- 50 Lee SC, Delikatny EJ, Poptani H, Pickup S, Glickson JD. *In vivo* (1)H MRS of WSU-DLCL2 human non-Hodgkin's lymphoma xenografts: response to rituximab and rituximab plus CHOP. *NMR Biomed* 2009; **22**: 259–65.